

ORIGINAL ARTICLE

Ahmed E. Ahmed · Sam Jacob · Beppino C. Giovanella
Antony J. Kozielski · Joachim G. Liehr
John S. Stehlin, Jr

Comparative disposition of the antineoplastic agent 9-nitro-camptothecin and the inactive isomer 12-nitro camptothecin in CASE-bearing nude mice: effect of route of administration on tissue distribution

Received: 22 November 1996 / Accepted: 4 April 1997

Abstract Purpose: 9-Nitrocamptothecin (9-NC) and 12-nitrocamptothecin (12-NC) are synthetic structural analogues of camptothecin (CPT) which have been prepared to explore the structure/activity relationship of this group of compounds against a wide variety of experimental tumors. As part of our investigation of the pharmacology and the mechanism of tumor inhibition of these compounds, we examined the effect of route of administration on the distribution of tritium-labeled 9-NC and 12-NC, an active and a poor chemotherapeutic agent, respectively. **Methods:** Quantitative whole-body autoradiography was used and our results were compared with previous results obtained with the parent compound CPT. **Results:** These studies revealed that, independent of the route of administration, both CPT derivatives were rapidly distributed to gall bladder, gastrointestinal tract and kidney. The excretion from these organs was indicated by the high levels of radioactivity in urine (urinary bladder) and feces (large intestines). The studies also indicated that the distributions of 9-NC and 12-NC were qualitatively similar, but quantitatively higher uptake of radioactivity was observed in animals treated with 12-NC than in those treated with 9-NC at 30 min following treatment. With the exception of the late sampling time (12 h after administration), the accumulation of radioactivity in the lungs (bronchioles) of animals that received an intravenous (i.v.) dose of 9-NC or 12-NC was higher than those

treated with an intramuscular (i.m.) dose. However, the retention of drug-derived radioactivity in the tumors of mice treated with an i.m. dose of 9-NC was higher than that in the tumors of i.v.-treated animals and was also higher than that in tumors of animals treated with 12-NC. **Conclusions:** These results suggest that higher accumulation of 9-NC in tumor tissues than of 12-NC may contribute to the more potent chemotherapeutic activity of the former agent. Our results also suggest that i.m. injection is a more effective route of administration than i.v. administration.

Key words Camptothecin analogues · Whole-body autoradiography · Tumor uptake · Route of administration · CASE · Disposition

Introduction

Camptothecin (CPT), 4(*S*)-4-ethyl-4-hydroxy-1H-pyrano[3, 4:6, 7]indolizino[1, 2-*b*]-quinoline-3,14[4-*H*, 12*H*]dione, a plant alkaloid, was isolated from *Camptotheca acuminata* Decne (Nyssaceae) [23]. CPT is an effective chemotherapeutic agent [1, 7, 14] used in the treatment of various human cancers xenografted into nude immunodeficient mice [5] and also in cancer patients as has been determined in a phase 1 trial [20]. The antitumor effect of CPT is thought to be based on its inhibition of DNA topoisomerase I [10, 16]. CPT is pharmacologically active, although most of the drug is rapidly excreted via the bile regardless of the route of administration [4]. In attempts to improve the therapeutic characteristics, many substituted CPT derivatives have been synthesized and examined for inhibition of topoisomerase I and antitumor activity in animals and humans. Minor chemical changes of the CPT molecule often result in marked alterations in the pharmacological activity [19].

In this study, we compared the uptake and distribution of a pharmacologically highly active CPT analogue, 9-nitrocamptothecin (9-NC), with those of an inactive isomer, 12-nitrocamptothecin (12-NC), to determine to

A.E. Ahmed (✉) · S. Jacob
Department of Pathology,
The University of Texas Medical Branch,
Galveston, TX 77555-0605, USA
Tel.: (409) 772-2877; Fax (409) 747-2429

J.G. Liehr
Department of Pharmacology and Toxicology,
The University of Texas Medical Branch,
Galveston, TX 77555-0605, USA

B.C. Giovanella · A.J. Kozielski · J.S. Stehlin, Jr
Stehlin Foundation for Cancer Research,
Houston, TX 77002, USA

what extent the differences in the biological activities of these substances were based on a differential exposure of the tumor to the cell-killing drug [15]. The pharmacokinetic characteristics of the two isomers were examined by whole body autoradiography (WBA) of tumor-bearing animals treated with either radioactive 9-NC or 12-NC by intramuscular (i.m.) or intravenous (i.v.) injection. The tumor used in these experiments was a human colon carcinoma, CASE, xenografted into "nude" immunodeficient mice [9, 21] in an analogous manner to previous studies with CPT [4]. The same experimental tumor system was used to permit a comparison of the pharmacokinetic characteristics of substituted CPT derivatives with those of the parent drug studied previously [4]. Our results demonstrate that the pharmacologic activities of substituted derivatives of CPT may be dependent on uptake of the drug by the tumor in addition to other characteristics examined previously such as inhibition of topoisomerase I.

Materials and methods

Chemicals

CPT, purchased from Good Land Enterprises, Vancouver, B.C., Canada, was converted to 9-NC and 12-NC as described previously [19]. 9-NC and 12-NC were isolated and purified by chromatography as described previously [13]. [^3H]-labeled 9-NC and 12-NC were synthesized by Moravek Biochemicals, Brea, Calif., using a gaseous [^3H] exchange procedure. The stability of CPT and its derivatives labeled by this procedure at the C-12 position has been examined previously [13]. Tritium loss occurs in vivo and in vitro with a half-life of 16.5 h [13].

The specific activity of the dosing solution was determined in PCS Scintillation Fluor (Amersham) using a Beckman LS 7500

scintillation counter. Counting efficiency was determined using external standardization. All other chemicals and reagents used were of the highest purity commercially available and all experiments were conducted in a well-ventilated hood using the appropriate precautions.

Animals and tumor implantation

Swiss immunodeficient (nude) mice (weighing 30–35 g) of the NIH-1 high-fertility strain were bred and maintained under strict pathogen-free conditions in our laboratory and were used for these experiments [11]. The human tumor used for this experiment was colon carcinoma CASE [8, 12]. This tumor is totally resistant to most conventional anticancer drugs [8, 17], but is sensitive to CPT and its derivatives [17, 22, 23]. Human malignant tumors were transplanted into mice by inoculating 50 mg of finely minced tumor tissue in 0.5 ml Eagle's minimum essential medium (GIBCO, Long Island, N.Y.) under the skin of the dorsal chest region. [^3H]-labeled 9-NC or 12-NC treatment was started 10 days after inoculation when tumors had grown to a size of approximately 1.5 cm diameter.

Animal treatment

[^3H]-9-NC or [^3H]-12-NC were administered i.v. into the tail vein or i.m. into the femoral muscle of tumor-bearing mice (three animals per group) as a fine suspension (20%) in Intralipid (Kabil Vitrum, Alameda, Calif.) as described previously in experiments with CPT [4]. Each mouse received 2 mg/kg 9-NC with an activity of 60 μCi /mouse or 2 mg/kg 12-NC with an activity of 100 μCi /mouse irrespective of the route of administration. This volume has been shown previously to be well tolerated and to cause no apparent ill-effects to treated animals [4].

Whole-body autoradiography

WBA was carried out by a modification of the method of Ullberg [22]. Briefly, treated animals were sacrificed by CO_2 anoxia 30 min,

Table 1 Distribution of radioactivity (nCi/g tissue) in organs and tumors of CASE-bearing nude mice as determined by computer-assisted image analysis following a single i.m. injection of 2 mg/kg

(equivalent to 300 μCi /kg) [^3H]-9NC or [^3H]-12NC. Values are means \pm SD of selected autoradiograms (*n.i.* organ not identified in the section analyzed)

Organ	30 min		2 h		12 h	
	9-NC	12-NC	9-NC	12-NC	9-NC	12-NC
Heart/blood	2.2 \pm 0.4	4.4 \pm 1	3.5 \pm 0.4	1.7 \pm 0.2	1.2 \pm 0.4	0.9 \pm 0.1
Eye	1.5 \pm 0.3	2.4 \pm 0.1	3.4 \pm 0.4	0.4 \pm 0.01	0.8 \pm 0.04	0.2 \pm 0.01
Lacrimal gland	4.2 \pm 0.2	7.9 \pm 1	5.3 \pm 0	4.6 \pm 0.2	0.5 \pm 0.01	n.i.
Hardarian gland	4.1 \pm 0.5	6.7 \pm 0.7	4.0 \pm 0.8	n.i.	2.3 \pm 0.01	1.0 \pm 0.01
Bone marrow	3.1 \pm 0.5	4.6 \pm 0.5	5.3 \pm 0.9	1.1 \pm 0.01	1.7 \pm 0.3	1.0 \pm 0.01
Tumor	3.7 \pm 0.5	5.5 \pm 0.8	5.5 \pm 0.4	1.1 \pm 0.2	1.6 \pm 0.3	1.0 \pm 0.02
Brain/spinal cord	0.7 \pm 0.2	1.1 \pm 0.03	3.3 \pm 0.9	0.3 \pm 0.01	0.5 \pm 0.01	0.2 \pm 0.01
Liver	10.9 \pm 3	34.6 \pm 3	7.2 \pm 1	6.0 \pm 0.9	3.7 \pm 0.9	1.8 \pm 0.3
Lung	2.5 \pm 0.6	5.3 \pm 1	3.5 \pm 0.3	2.2 \pm 0.2	1.2 \pm 0.2	1.0 \pm 0.3
Spleen	3.1 \pm 0.7	6.2 \pm 0.3	n.i.	5.4 \pm 0.7	n.i.	0.7 \pm 0.1
Renal pelvis	33.7 \pm 8	6.2 \pm 0.9	14.2 \pm 0.5	n.i.	2.8 \pm 0.1	n.i.
Renal cortex	8.7 \pm 1	14.0 \pm 2	5.8 \pm 0.4	5.0 \pm 0.8	2.4 \pm 0.9	1.0 \pm 0.1
Gallbladder	90.9 \pm 18	115.6 \pm 17	69.7 \pm 6	107.5 \pm 7	36.1 \pm 7	n.i.
Stomach contents	21.2 \pm 4	5.0 \pm 1	39.4 \pm 4	31.6 \pm 0.5	2.4 \pm 0.8	3.5 \pm 0.8
Stomach mucosa	3.8 \pm 0.5	6.1 \pm 0.2	4.6 \pm 0.2	5.7 \pm 0.4	0.9 \pm 0.1	1.4 \pm 0.02
Small intestinal contents	71.3 \pm 9	42.6 \pm 8	91.6 \pm 8	102.8 \pm 10	8.4 \pm 0.5	n.i.
Small intestinal mucosa	13.3 \pm 5	6.3 \pm 0.8	11.5 \pm 0.5	8.1 \pm 3	2.3 \pm 0.5	3.0 \pm 0.9
Large intestinal contents	11.1 \pm 1	7.9 \pm 1	21.2 \pm 3	75.8 \pm 13	12.0 \pm 1	9.1 \pm 1
Large intestinal mucosa	9.5 \pm 2	6.3 \pm 0.8	8.0 \pm 1	10.1 \pm 0.3	4.5 \pm 0.8	2.2 \pm 0.03
Urinary bladder	74.1 \pm 11	53.3 \pm 12	n.i.	80.0 \pm 4	38.6 \pm 2	29.4 \pm 5
Site of injection	71.1 \pm 6	48.9 \pm 9	60.9 \pm 7	24.2 \pm 1	45.7 \pm 3	58.8 \pm 7

2 h or 12 h following administration of either of the drugs. Carcasses were immediately immersed in a hexane/dry-ice mixture at -70°C for about 5 min to achieve flash freezing. Frozen carcasses were embedded in carboxymethyl cellulose gel. The gel containing a carcass was again immersed in a hexane/dry-ice mixture at -70°C for 15 min and stored at -20°C , until the time of sectioning. Multiple sagittal sections of 30 μm thickness were then cut with a cryomicrotome (LKB PMV 2250) maintained at -20°C . Animal sections in which several organs could easily be identified, were mounted on scotch tape 800 (3M Co; St. Paul, Minn.). For autoradiography, Amersham Ultra film (Amersham Industries, Chicago, Ill.) was placed on the mounted animal sections for 6–8 weeks along with precalibrated [^3H] reference strips (Microscales; Amersham, Chicago, Ill.). The films were processed at different exposure times ranging from 5 to 8 weeks to compensate for the saturation of radioactivity on the film.

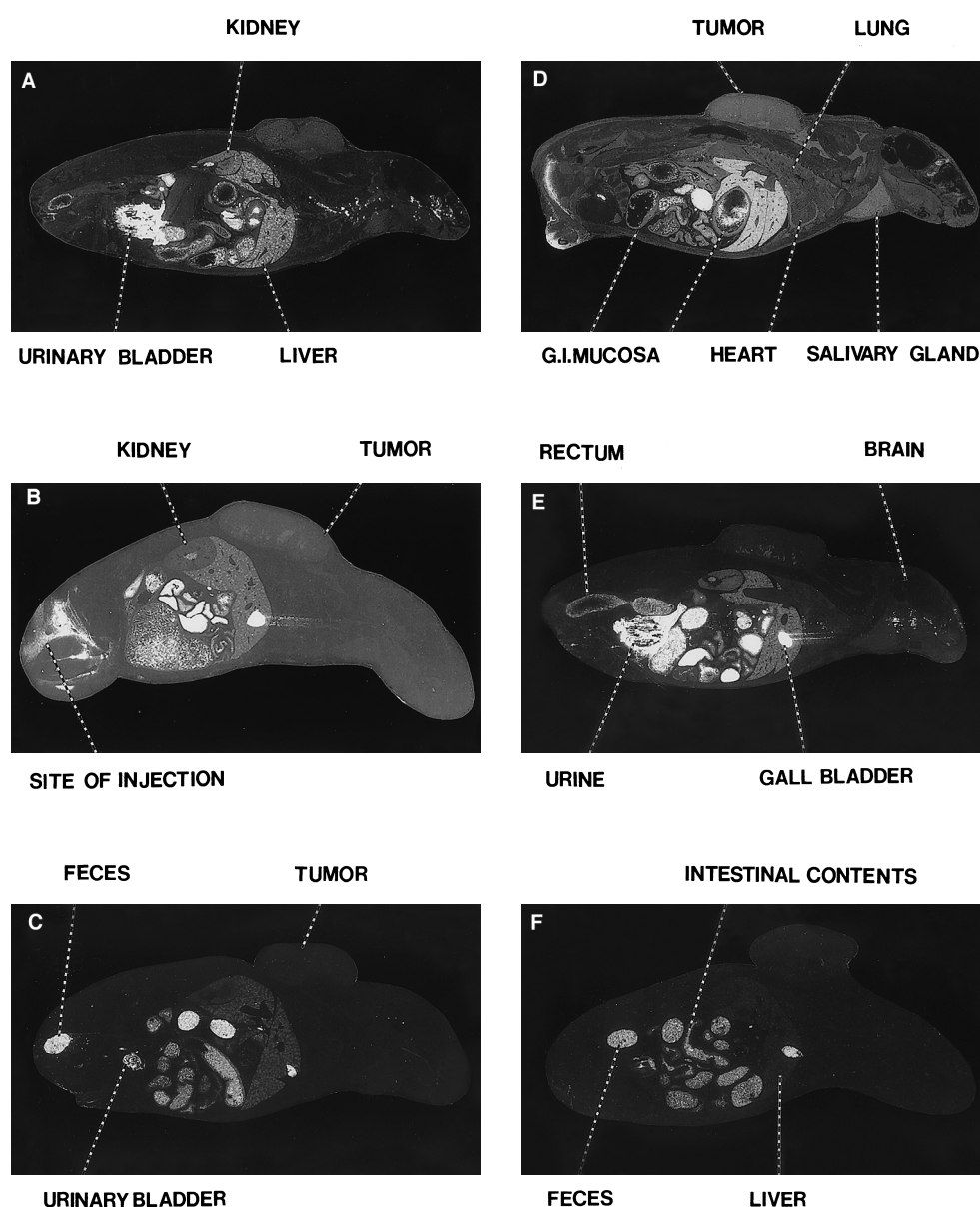
Representative autoradiographs were used as negatives for the production of photographs. Therefore, in the figures presented, white areas represent sites of high radioactive uptake. The gray to black intensities represent sites of medium to low levels of radioactivity.

Computer-assisted image analysis of WBA

The distribution patterns of [^3H]-9-NC and [^3H]-12-NC were quantitatively determined using computer-assisted image analysis of the autoradiographs [3]. Autoradiographs were selected and the maximum number of organs anatomically identifiable were studied in detail. Several samples representing different areas of an organ were picked from these autoradiographs to evaluate the distribution of radioactivity. Optical densities for different organs in these autoradiographs were determined with an autoscanning image analyzer (MCID), manufactured by Imaging Research, Brock University (St. Catherine, Canada). Briefly, a response curve relating the level of activity with the digitized number (an arbitrary number produced by the video camera) was constructed by digitizing a step-wise series of autoradiographed radioisotopic standards. The computer used this information to calculate the actual amount of radioactivity in each pixel of the digitized matrix.

The final step in calculating the levels of activity in each pixel of the digitized image was performed by a polynomial fitting of the data to the standard calibration curve or by linear regression analysis. The quantified image was then displayed by coding 16

Fig. 1A–F A–C Whole-body autoradiographs of mice injected i.m. with [^3H]-9-NC (300 $\mu\text{Ci/kg}$) at (A) 30 min, (B) 2 h and (C) 12 h following administration, respectively. D–F Whole-body autoradiographs of mice injected i.m. with [^3H]-12-NC (300 $\mu\text{Ci/kg}$) at (D) 30 min, (E) 2 h and (F) 12 h following administration, respectively



different levels of activity. Regions of interest were then selected by using the MCID system to analyze the autoradiographs. Ten or more pixels from each region or tissue were sampled, digitized, and converted to nanocuries per gram tissue using the calibrated autoradiographic standard curve. From these values, the means and standard deviations were calculated. Total blood values were determined in cardiac cavities and/or in the abdominal aorta.

The distribution coefficients (the tissue:blood ratios) of [^3H]-9-NC or [^3H]-12-NC in the organs were determined as described by Ahmed et al. [2].

Tumor uptake ratios

The uptake of [^3H]-labeled CPT derivatives in tumor compared to other tissues was determined by a method described by Fand et al. [6]. Nontumor tissues were selected based on the known pharmacokinetic properties of the drugs. The quantitative values obtained from computer-assisted image analysis were used for the determination of tumor:nontumor ratios.

Results

Distribution at 30 min after administration of [^3H]-9-NC or [^3H]-12-NC

Intramuscular

Higher levels of radioactivity accumulated in various tissues 30 min after i.m. administration of [^3H]-12-NC than after [^3H]-9-NC administration (Table 1). Both compounds were excreted via biliary and urinary pathways. However, the preferential excretion of 12-NC via liver and bile and the 9-NC via the kidneys and the

urinary bladder was evaluated by comparing the sums of radioactivity in the liver plus gallbladder vs. the renal pelvis plus urinary bladder (Table 1; Fig. 1A,D). However, 9-NC appeared to accumulate extensively in the acidic medium of the stomach. High amounts of radioactivity of [^3H]-9-NC were also detected in the liver, kidney and small intestinal mucosa. Intermediate levels of radioactivity were observed in the heart, lung, blood, bone marrow and the tumor (Table 1). Organs with comparable radioactivity derived from the two drugs were the tumor, heart muscle, salivary gland, bone marrow, lacrimal gland and gastrointestinal mucosa. Low levels of ^3H uptake were observed in the lung and blood vessels.

Intravenous

A pattern of higher levels of uptake of radioactivity from [^3H]-12-NC than from [^3H]-9-NC was observed 30 min after i.v. administration of the two drugs. Contrary to patterns observed following i.m. administration, [^3H]-9-NC was excreted preferentially via the liver and gallbladder into the intestinal contents, whereas [^3H]-12-NC followed the renal excretion pathway (renal pelvis and urinary bladder) (Table 2; Fig. 2A,D). Comparable levels of ^3H uptake from both compounds were observed in the brain/spinal cord, lung/bronchiole, and large intestinal mucosa. Low levels of accumulation of radioactivity were observed in the lung, heartblood and bone marrow.

Irrespective of route of administration, animals treated with [^3H]-12-NC accumulated more radioactivity

Table 2 Distribution of radioactivity (nCi/g tissue) in organs and tumors of C57BL/6J mice as determined by computer-assisted image analysis following a single i.v. injection of 2 mg/kg

(300 $\mu\text{Ci/kg}$) [^3H]-9NC or [^3H]-12NC. Values are means \pm SD nCi/g tissue of selected autoradiograms (n.i. organ not identified in the sections analyzed)

Organ	30 min		2 h		12 h	
	9-NC	12-NC	9-NC	12-NC	9-NC	12-NC
Heart/blood	1.2 \pm 0.2	5.2 \pm 0.5	1.2 \pm 0.2	1.7 \pm 0.3	1.2 \pm 0.02	0.6 \pm 0.02
Eye	0.8 \pm 0.1	1.3 \pm 0.02	0.8 \pm 0.1	1.4 \pm 0.02	1.4 \pm 0.02	n.i.
Lacrimal gland	2.9 \pm 0.6	6.8 \pm 0.1	2.4 \pm 0.3	4.6 \pm 0.03	n.i.	n.i.
Hardarian gland	2.2 \pm 0.3	n.i.	2.2 \pm 0.3	n.i.	n.i.	n.i.
Bone marrow	1.5 \pm 0.3	5.0 \pm 0.5	1.4 \pm 0.3	1.1 \pm 0.2	0.7 \pm 0.2	0.4 \pm 0.01
Tumor	2.2 \pm 0.3	6.1 \pm 0.1	2.2 \pm 0.4	2.7 \pm 1	0.9 \pm 0.2	0.5 \pm 0.1
Brain/spinal cord	0.7 \pm 0.1	0.9 \pm 0.01	0.7 \pm 0.2	0.4 \pm 0.02	0.6 \pm 0.1	0.4 \pm 0.02
Liver	5.4 \pm 0.9	11.6 \pm 2	4.3 \pm 0.2	5.6 \pm 0.2	2.9 \pm 0.2	2.7 \pm 0.6
Lung	2.1 \pm 0.6	6.5 \pm 1	2.1 \pm 0.6	2.2 \pm 0.3	1.6 \pm 0.1	2.2 \pm 0.1
Lung/bronchiole	56.0 \pm 12	62.8 \pm 9	32.1 \pm 8	53.1 \pm 6	12.0 \pm 0.5	45.3 \pm 7
Spleen	n.i.	7.8 \pm 2	n.i.	5.4 \pm 0.7	n.i.	3.2 \pm 0.3
Renal pelvis	7.7 \pm 1	48.8 \pm (18)	6.2 \pm 0.2	n.i.	4.5 \pm 0.5	n.i.
Renal cortex	3.2 \pm 0.4	11.2 \pm 0.5	3.1 \pm 0.4	4.8 \pm 0.6	1.5 \pm 0.5	0.9 \pm 0.03
Gallbladder	113.8 \pm 14	99.7 \pm 9	123 \pm 17	90.8 \pm 8	20.9 \pm 2	17.0 \pm 2
Stomach contents	1.0 \pm 0.2	3.9 \pm 0.8	1.0 \pm 0.3	32.9 \pm 4	1.9 \pm 0.01	5.5 \pm 0.7
Stomach mucosa	2.1 \pm 0.1	7.5 \pm 0.5	2.1 \pm 0.3	5.7 \pm 1	1.0 \pm 0.2	n.i.
Small intestinal contents	88.8 \pm 15	47.4 \pm 7	59.3 \pm 8	99.8 \pm 11	3.4 \pm 0.9	n.i.
Small intestinal mucosa	5.2 \pm 1	11.9 \pm 0.5	4.3 \pm 1	8.1 \pm 0.5	1.9 \pm 0.2	2.4 \pm 0.1
Large intestinal contents	41.2 \pm 11	27.7 \pm 2	32.8 \pm 0.8	65.3 \pm 8	9.4 \pm 1	17.0 \pm 0.5
Large intestinal mucosa	5.4 \pm 1	6.9 \pm 0.3	3.9 \pm 0.6	9.3 \pm 0.3	3.4 \pm 2	2.9 \pm 0.2
Urinary bladder	56.2 \pm 13	80.0 \pm 8	59.8 \pm 7	69.8 \pm 10	n.i.	27.2 \pm 0.3

than those treated with [^3H]-9-NC especially in the liver, kidney and the tumor. A major difference in the distribution as a function of route of administration was the spotty accumulation of radioactivity in the lungbronchioles of animals treated with an i.v. dose of both analogues. Brain, spinal cord and testis showed the least radioactivity in all experiments at this time point.

Distribution at 2 h after administration of [^3H]-9-NC or [^3H]-12-NC

Intramuscular

Higher levels of radioactivity from [^3H]-9-NC were detected in most organs including the tumor 2 h after i.m. administration of both drugs (Table 1 Fig. 1B,E). Moreover, the stomach continued to accumulate high

levels of [^3H]-9-NC at this time point. These compounds followed the preferential excretion patterns already observed after 30 min, i.e. 9-NC via the renal pelvis and urine and 12-NC via the liver and gallbladder into the intestine.

Intravenous

In contrast to the pattern observed after i.m. administration, levels of radioactivity from [^3H]-9-NC in most organs including tumor tissue were lower than those from [^3H]-12-NC 2 h after i.v. administration (Table 2; Fig. 2B,E). Moreover, hepatic radioactivity levels of the two drugs were comparable, in contrast to the differences observed after i.m. administration. Furthermore, the uptake of [^3H]-12-NC by lung was almost twice that and by stomach contents 32 times that of [^3H]-9-NC (Table 2).

Fig. 2A–F A–C Whole-body autoradiograms of mice injected i.v. with [^3H]-9-NC (300 $\mu\text{Ci/kg}$) at (A) 30 min, (B) 2 h and (C) 12 h following administration, respectively. D–F Whole-body autoradiograms of mice injected i.v. with [^3H]-12-NC (300 $\mu\text{Ci/kg}$) at (D) 30 min, (E) 2 h and (F) 12 h following administration, respectively

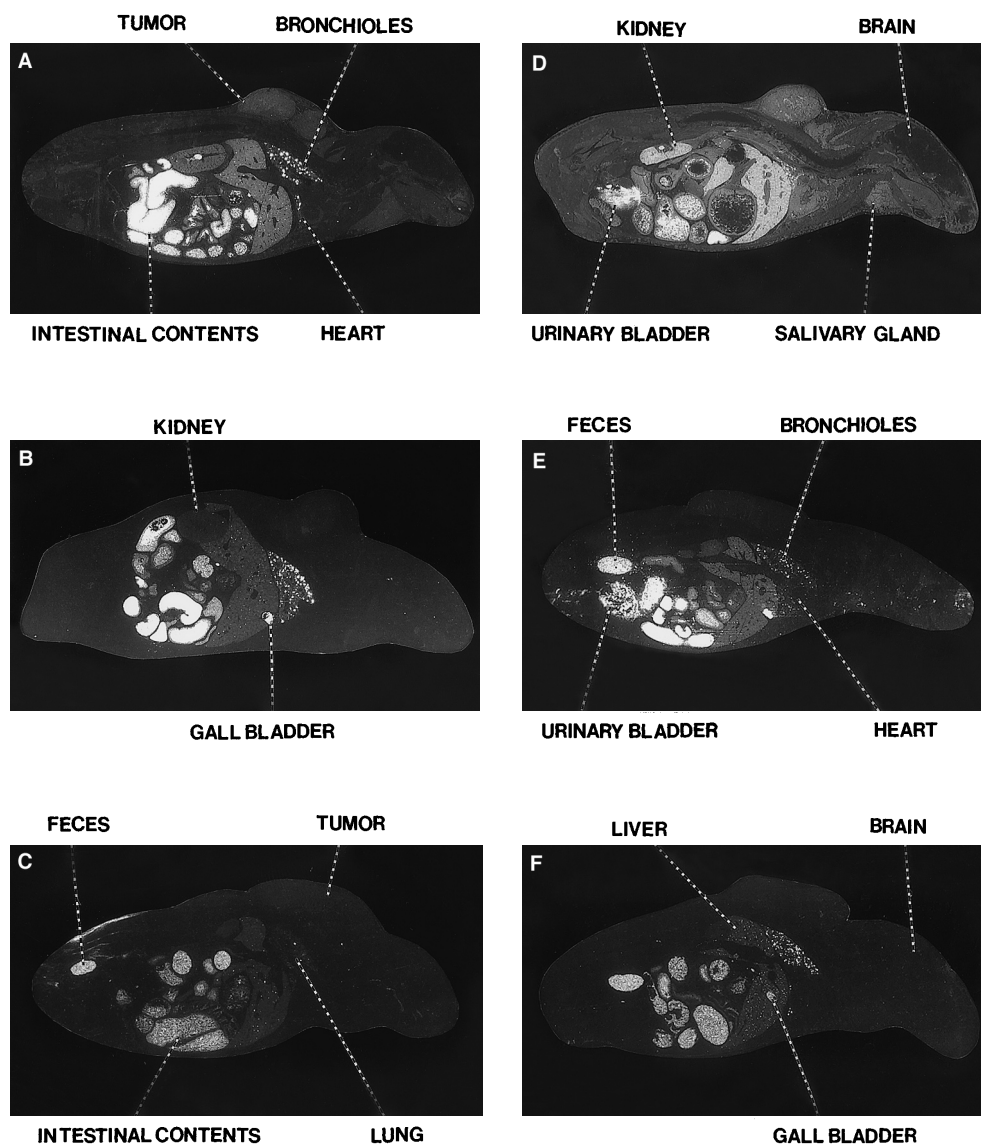


Table 3 Distribution coefficients (tissue:blood [^3H] radioactivity ratios, nCi) following a single i.m. or i.v. injection of 2 mg/kg (equivalent to 300 $\mu\text{Ci/kg}$) [^3H]-9-NC or [^3H]-12-NC into CASE-

bearing nude mice. Values are means of two animals (*n.i.* organ not identified in section analyzed)

Organ	i.m.						i.v.					
	30 min		2 h		12 h		30 min		2 h		12 h	
	9-NC	12-NC	9-NC	12-NC	9-NC	12-NC	9-NC	12-NC	9-NC	12-NC	9-NC	12-NC
Heart/blood	1.0	1.0	1.0	1.0	1.0	1.0	1.0	1.0	1.0	1.0	1.0	1.0
Tumor	1.7	1.2	1.6	0.6	1.1	1.1	1.8	1.2	1.8	1.5	0.8	0.8
Eye	0.7	0.5	1.0	0.2	0.7	0.2	0.7	0.3	0.7	0.9	1.1	n.i.
Lacrimal gland	1.9	1.8	1.5	0.6	2.4	n.i.	2.4	1.3	2.4	2.7	n.i.	n.i.
Hardarian gland	1.8	1.5	1.1	n.i.	1.9	1.1	1.8	n.i.	1.8	n.i.	n.i.	n.i.
Bone marrow	1.4	1.0	1.5	0.6	1.4	1.2	1.2	0.9	1.1	0.6	0.6	0.7
Brain/spinal cord	0.3	0.2	0.9	0.2	0.4	0.2	0.6	0.1	0.5	0.2	0.5	0.7
Liver	5.0	3.3	2.1	3.5	3.0	2.0	4.5	2.2	3.6	3.3	2.4	4.5
Gallbladder	41	26	19	63	30	n.i.	94	19	102	53	17	28
Lung	1.1	1.2	1.0	1.3	1.2	1.1	1.8	1.2	1.7	1.3	1.3	3.6
Lung/bronchiole	n.i.	n.i.	n.i.	n.i.	n.i.	n.i.	46	12	26	31	10	75
Renal cortex	3.9	3.2	1.6	2.9	2.0	1.1	2.7	2.1	2.6	2.8	1.2	1.5
Stomach mucosa	1.7	1.3	1.3	3.3	0.8	1.5	1.8	1.4	1.7	3.3	0.8	n.i.
Small intestinal mucosa	6.0	1.4	1.2	4.7	1.9	3.3	4.3	9.1	3.5	4.7	1.6	n.i.
Large intestinal mucosa	4.3	1.4	2.2	5.9	3.7	2.4	4.5	1.3	3.2	5.4	3.2	4.8
Urinary bladder	33.6	12	n.i.	47	32.1	32	46	15	49	41	n.i.	45

Distribution at 12 h after administration of [^3H]-9-NC or [^3H]-12-NC

NC retained slightly more radioactivity 12 h after treatment than those of mice treated with [^3H]-12-NC.

Higher levels of radioactivity from [^3H]-9-NC than from [^3H]-12-NC were retained in most tissues including in the tumor 12 h after i.m. or i.v. administration (Tables 1, 2; Figs. 1C,F; 2C,F). The excretion of radioactivity continued to follow the patterns observed 30 min after administration of the two drugs. At this time point, the highest levels of radioactivity of [^3H]-12-NC were detected in lung and bronchiole tissue.

Generally, the retention of radioactivity derived from both CPT analogues was similar. The spotty appearance of the lung indicated a high drug concentration in pulmonary bronchioles following i.v. administration of both drugs. The tumors of animals treated with [^3H]-9-

Distribution coefficients

Table 3 shows the distribution coefficients (tissue/blood) of radioactivity in organs of mice treated with the drugs. The tumor uptake ratios were higher than those of the blood under all experimental conditions except at 12 h after administration of the drugs. Organs with very high distribution coefficients were the gallbladder, lungbronchioles, urinary bladder, renal cortex, and intestinal mucosa. The high distribution coefficients in the gallbladder, urinary bladder, lung and intestinal mucosa may be predictive of drug toxicities in these organs.

Table 4 Tumor:tissues ratios derived from computer-assisted image analysis following a single i.m. or i.v. injection of 2 mg/kg (equivalent to 300 $\mu\text{Ci/kg}$) [^3H]-9-NC or [^3H]-12-NC to CASE-

bearing nude mice. Values are means \pm SD of at least 12 autoradiographic analyses selected from two mice (*n.i.* organ not identified in sections analyzed)

	i.m.						i.v.					
	30 min		2 hr		12 hr		30 min		2 hr		12 hr	
	9-NC	12-NC	9-NC	12-NC	9-NC	12-NC	9-NC	12-NC	9-NC	12-NC	9-NC	12-NC
Tumor/Blood	1.7	1.3	1.5	0.6	1.3	1.1	1.8	1.2	1.8	1.6	0.7	0.7
Tumor/bone marrow	1.1	1.2	1.0	1.0	0.9	1.0	1.4	1.3	1.6	2.4	1.3	1.3
Tumor/lung	1.5	1.0	1.5	0.5	1.3	1.0	1.0	0.9	1.0	1.2	0.6	0.6
Tumor/brain	5.2	5.0	1.6	3.3	3.2	5.0	3.1	6.7	3.1	9.0	1.5	1.5
Tumor/liver	0.3	0.4	0.7	0.2	0.4	0.5	0.4	0.5	0.5	0.4	0.3	0.3
Tumor/gallbladder	0.04	0.04	0.07	0.01	0.04	n.i.	0.01	0.06	0.01	0.03	0.04	0.04
Tumor/gastric contents ^a	0.1	0.2	0.1	0.01	0.2	0.1	0.05	0.2	0.07	0.04	0.18	0.18

^aValues of gastric contents include stomach, small and large intestines

Moreover, the higher distribution coefficients in the gallbladder and urinary bladder reflect the high rates of excretion of these compounds irrespective of the route of administration.

Tumor/nontumor tissue ratios

The tumor/nontumor ratios derived from computer-assisted image analysis following a single i.m. or i.v. dose of [^3H]-9-NC or [^3H]-12-NC are shown in Table 4. These ratios demonstrate that gastric and gallbladder contents had much higher levels of radioactivity than the tumor under all experimental conditions, again indicating the high rates of elimination of the two drugs. Radioactivity in the tumor was higher than in the blood following i.m. and i.v. administration of [^3H]-9-NC or [^3H]-12-NC except at 12 h after i.v. administration of the drugs and 2 h after i.m. administration of [^3H]-12-NC. In other tissues, such as bone marrow, the concentrations of drug differed little from those of the peripheral blood.

Discussion

Our studies (Table 4) demonstrate a higher uptake (tissue/blood) of 9-NC and a prolonged retention of this drug by tumor tissue compared with the pharmacologically inactive isomer 12-NC. This difference in drug accumulation by tumor tissue was particularly pronounced following i.m. injection. Nevertheless, this differential drug uptake and retention may contribute to, but cannot be the sole explanation of, the differences in chemotherapeutic activities of these two CPT derivatives. This conclusion is consistent with inherent differences in pharmacological activities of 9-NC and 12-NC, which are demonstrated by their differential cytotoxicities in cell culture [18] and which may be based on differences in their interactions with topoisomerase I.

Our results demonstrate that following i.m. administration, 12-NC was transported preferentially via liver and bile, whereas 9-NC was excreted mainly via the renal pelvis into the urine. In contrast, i.v. administration of 9-NC resulted in the preferential excretion via the gallbladder and intestine, whereas 12-NC followed the renal excretion pathway. The higher retention of 9-NC after i.m. injection points to this route as the preferred pathway of administration. These results are consistent with previous results with the parent substance CPT, which have identified i.m. and also oral administration as better administration routes for CPT and its derivatives than i.v. infusion [4]. Moreover, the decreases in tumor: blood concentration ratios 12 h after injection of both drugs indicate that more frequent administration of smaller doses is preferred to less frequent administration of larger doses.

The pattern of distribution of 9-NC did not differ markedly from that of 12-NC nor from that of the parent compound CPT published previously [4]. The

apparent lack of pronounced differences in the distribution pattern of CPT and its derivatives is consistent with structural characteristics rather than differential target organ concentrations being the basis of differences in chemotherapeutic activity of the various CPT derivatives as mentioned above. The similar distribution pattern of members of this class of drugs also suggests that their distribution and disposition is mainly influenced by the five-membered ring structure of the parent alkaloid.

Gastrointestinal toxicity of CPT and its analogues has been reported in animal and human studies, which includes thickening of the walls of the gallbladder and cholecystitis [20]. In addition, cystitis of the urinary bladder is a frequent toxic side effect of CPT and 9-NC in cancer patients. The high drug concentrations in the urinary bladder, gallbladder and intestinal contents reported for the nitro derivatives in this study and for CPT previously [4] are consistent with the induction of toxic side effects at these sites. In addition, the i.v. treatment of patients may pose toxicity risks to the lung as demonstrated by the high accumulation of the nitro derivatives in pulmonary bronchioles at all time points.

The accumulation of i.m.-administered 9-NC in the acidic stomach contents may represent a site of accumulation of this drug in the therapeutically active lactone form. The lactone form of CPT and derivatives has previously been shown to be formed under acidic conditions [24].

The accumulation of CPT derivatives in the stomach, intestines and pulmonary bronchioles points to a high therapeutic potential of 9-NC and possibly other CPT derivatives in the treatment of cancers of the colon, stomach, intestines and lung. In the treatment of these diseases, the stomach and the gallbladder may serve as reservoirs for the internal infusion of the drug to tumor tissues. The antitumor activity of 9-NC in humans is currently being explored in clinical trials.

Acknowledgement We thank Ms. Dora Salinas for preparing the manuscript.

References

1. Abbot BJ (1976) Bioassay of plant extracts for anticancer activity. *Cancer Treat Rep* 60: 1007
2. Ahmed AE, Jacob S, Loh J-P (1991) Studies on the mechanism of haloacetonitrile toxicity: quantitative whole body autoradiographic distribution of 2-[^{14}C]-chloroacetonitrile in rats. *Toxicology* 67: 279
3. Ahmed AE, Jacob S, Au WW (1994) Quantitative whole body autoradiographic disposition of glycol ether in mice: effect of route of administration. *Fundam Appl Toxicol* 22: 266
4. Ahmed AE, Jacob S, Giovannella BC, Kozielski AJ, Stehlin JS Jr, Liehr JG (1996) Influence of route of administration of (^3H)-camptothecin distribution and tumor uptake in CASE-bearing nude mice: whole-body autoradiographic studies. *Cancer Chemother Pharmacol* 39: 122
5. DeWys WD, Humphreys SR, Goldin A (1968) Studies on the therapeutic effectiveness of drugs with tumor weight and survival time indices of Walker 256 carcinosarcoma. *Cancer Chemother Rep* 52: 229

6. Fand I, Sharkey RM, McNally WP, Brill AB, Som P, Yamamoto K, Primus FJ, Goldenberg DM (1986) Quantitative whole-body autoradiography of radiolabeled antibody distribution in a xenografted human cancer model. *Cancer Res* 46: 271
7. Gallo RC, Whang-Peng J, Adamson RH (1971) Studies on the antitumor activity, mechanism of action and cell cycle effects. *J Natl Cancer Inst* 46: 789
8. Giovanella BC, Stehlin JS (1973) Heterotransplantation of human malignant tumors in "nude" thymusless mice. I. Breeding and maintenance of "nude" mice. *J Natl Cancer Inst* 51: 615
9. Giovanella BC, Stehlin JS, Shepard RC, Williams LJ (1983) Correlation between response to chemotherapy of human tumors in patients and in nude mice. *Cancer* 52: 1146
10. Giovanella BC, Stehlin JS, Wall ME, Wani MC, Nicholas AW, Liu LF, Silber R, Potmesil M (1989) DNA topoisomerase I targeted chemotherapy of human colon cancer in xenografts. *Science* 246: 1046
11. Giovanella BC, Hinz HR, Kozielski AJ, Stehlin JS, Silber R, Potmesil M (1991) Complete growth inhibition of human cancer xenografts in nude mice by treatment with 20(S) camptothecin. *Cancer Res* 51: 3052
12. Govindachari TR, Viswanathan N (1972) 9-Methoxy camptothecin. A new alkaloid from *mappia foetida* Miers. *Indian J Chem* 10: 453
13. Hinz HR, Harris NJ, Giovanella BC, Ezell EL, Liehr JG (1996) Stabilities of ^3H - and ^2H -labelled camptothecins. *Labelled Compounds Radiopharm* 38: 733
14. Leibovitz A, Stinson JC, McCombs III WB, McCoy LE, Mazur VC, Mabry ND (1976) Classification of human colorectal adenocarcinoma cell lines. *Cancer Res* 36: 4562
15. Li LH, Fraser TJ, Olin EJ, Bhuyan BK (1972) Action of camptothecin on mammalian cells in culture. *Cancer Res* 32: 2643
16. Liu LF (1989) DNA topoisomerase poisons as antitumor drugs. *Annu Rev Biochem* 58: 351
17. Moore BG, Schwartz HS, Hodo H (1970) Inhibition of macromolecular synthesis in L1210 ascites tumor cells by camptothecin (abstract) *J Cell Biol* 47 (Part 2): 144A
18. Pantazis P, Hinz HR, Mendoza JT, Kozielski AJ, Williams Leo J Jr, Stehlin JS Jr, Giovanella BC (1992) Complete inhibition of growth followed by death of human malignant melanoma cells in vitro and regression of human melanoma xenografts in immunodeficient mice induced by camptothecins. *Cancer Res* 52: 3980
19. Sawada S and Yokokura T (1996) Synthesis of CPT-11 (irinotecan hydrochloride trihydrate). *Ann NY Acad Sci* 803: 13–28
20. Stehlin JS, Natelson EA, Hinz HR, Giovanella BC, de Ipolyi PD, Fehir KM, Trezona TP, Vardeman DM, Harris NJ, Marcee AK, Kozielski AJ, Ruiz-Razura A (1995) Phase I clinical trial and pharmacokinetics resulted with oral administration of 20(S)-camptothecin. In: Potmesil M, Pinedo H (eds) *Camptothecins: new anticancer agents*. CRC Press, Boca Raton, pp 59–65
21. Tafur S, Nelson JD, DeLong DC, Svoboda GH (1976) Antiviral components of *Ophiorrhiza mungos* isolation of camptothecin and 10-methoxy-camptothecin. *Lloydia* 39: 261
22. Ullberg S (1977) The technique of whole-body autoradiography. Cryosectioning of large specimens (special issue on whole-body autoradiography). *Science tools, the LKB Instrument Journal*, Uppsala, Sweden, pp 2–29
23. Venditti JM, Abbot BJ (1967) Studies on oncolytic agents from natural sources. Correlations of activity against animal tumors and clinical effectiveness. *Lloydia* 30: 332
24. Wall ME, Wani MC, Cook CE, Palmer KH, McPhail AT, Sim GA (1966) Plant antitumor agents I. The isolation and structure of camptothecin, a novel alkaloidal tumor inhibitor from *camptotheca acuminata*. *J Am Chem Soc* 88: 3888